Environ Monit Assess (2014) 186:1063–1081
DOI 10.1007/s10661-013-3439-1

Modified Grey Model and its application to groundwater flow analysis with limited hydrogeological data: a case study of the Nubian Sandstone, Kharga Oasis, Egypt

Wael Elham Mahmod · Kunio Watanabe

Received: 25 January 2013 / Accepted: 14 September 2013 / Published online: 4 October 2013

Abstract Groundwater flow at Kharga Oasis, located in the western desert of Egypt, was previously analyzed using numerical models; however, the lack of basic data often limits the implementation of these models, as well as introducing a problem for model calibration and validation. The Grey Model (GM) was used to overcome these difficulties of data limitation and uncertainty of hydrogeological conditions. However, no clear theories exist for selecting the number of input model trends and the most suitable values of input parameters. Therefore, in the current study, a modification of the GM is newly proposed and called the Modified Grey Model (MGM) in an attempt to determine a process for selecting the best input models' trends with the appropriate values of input parameters to achieve acceptable fitting to observations. The sensitivity analysis results showed that the MGM produced more stable results than the GM using a wide range of values for input parameters. Moreover, the MGM reduced the calculation time required for fitting the measured piezometric level trends by 99.8 %. Three development scenarios of groundwater withdrawal were proposed that involved either expanding the present extraction rate or redistributing the groundwater withdrawal over the recent working production wells (RWPWs). The results concluded that the groundwater table in the northern part of the oasis could be temporally recovered to an economical piezometric level; however, the table in the southern part is severely decreased. Therefore, new production wells are recommended to be constructed in the southern part far enough from the RWPWs.

Keywords Nubian Sandstone Aquifer System · Groundwater management · Kharga Oasis · Egypt · Grey Model · Modified Grey Model

W. E. Mahmod (✉) · K. Watanabe
Geo-sphere Research Institute, Department of Civil and Environmental Engineering, Saitama University, 255, Shimo Okubo, Sakura-Ku,
Saitama City, Saitama 338-8570, Japan
e-mail: wdpp20010@yahoo.com

K. Watanabe
e-mail: kunio@mail.saitama-u.ac.jp

Introduction

Kharga Oasis is the capital of the New Valley Governorate, which includes the western desert of Egypt; it is also one of the largest oases in Africa. There are four major oases in the New Valley: Kharga, Farafra, Dakhla, and Baris Oases. The Nubian Sandstone Aquifer System (NSAS) extends under the New Valley area and acts as a major water resource. Heinl and Thorweihe (1993) reported that the groundwater in this aquifer is non-renewable and is shared among Egypt, Libya, Sudan, and Chad. The total area of the aquifer covers over 630,000 km^2, and the bottom of this aquifer reaches to a depth of 3.5 km below the surface in some areas (Ebraheem et al. 2002). Although it is a huge water resource, the groundwater level in Kharga has been severely decreased due to recent agricultural and

industrial development. Hence, an effective management system of the groundwater withdrawal is strongly needed in this area.

The numerical analysis and simulation of groundwater flow is an effective tool for constructing a proper management system. For this purpose, many researchers have investigated the hydrogeological conditions of the NSAS and analyzed the groundwater flow using different numerical models. These studies can be generally divided into two types based on the size of the area treated. Ebraheem et al. (2002) and Heinl and Thorweihe (1993) performed numerical analyses over a wide regional area, covering not only Egypt but also neighboring countries, to analyze the flow in the whole NSAS. However, these analyses did not give sufficient information for smaller areas such as the Kharga Oasis. On the other hand, Nour (1996) analyzed the flow in a small area of the Kharga Oasis by assuming boundary conditions of flow and hydrogeological conditions. Although these analyses clearly presented the general tendency of groundwater flow, the models used included many problems with boundary conditions and the spatial distributions of hydraulic properties, such as hydraulic conductivity and storage coefficient. The Kharga Oasis in the western desert of Egypt is an arid area for which the hydrogeological data needed for groundwater simulation are lacking, thereby introducing a problem for model calibration and validation. The preceding discussion shows that it is difficult to develop a proper groundwater management system given such uncertainties and data limitations when using ordinary numerical models. A new model is therefore required to analyze groundwater flow when data are limited. Mahmod et al. (2013) have developed a new Grey Model (GM) as a proper technique for analyzing groundwater flow with limited data and uncertain hydrogeological conditions. The GM was combined with finite element method (FEM) and a linear regression model, which is based on genetic algorithms (GAs). FEM was used to analyze groundwater flow under the assumption of hydrogeological and boundary conditions to produce approximate solutions for temporal piezometric level changes. The GA model was used to fit the measured temporal piezometric level changes.

Although it was reported that the GM is a good tool for groundwater flow analysis, the model has no specific process for selecting the number of input piezometric level trends which reduce the uncertainty of fitting. This uncertainty comes from using models with a wide range of hydrogeological properties or using models that contain any calculation errors. Hence, it is difficult to select the GA input parameters that can achieve goodness of fit. The input piezometric level trends are the calculated ones from the assumed hydrogeological models. On the other hand, the input parameters are the parameters that are used to fit the measured observations such as Population Size, Crossover Probability, Mutation Probability, and Number of Generations. For simplicity, in the current study, the number of input piezometric level trends will be called the input models' trends. In the current study, a new methodology is introduced to establish a theory for selecting the input models' trends that produce the best fit to observations. The introduced method omits the models which cause noise of fitting and those that contain calculation errors. Hence, the proposed model can facilitate the selection of GA input parameters and consequently decreases the uncertainty of fitting to observations. In the following discussions, the new methodology is declared as Modified Grey Model (MGM). Moreover, the effect of the number of input models' trends in the values of input parameters was studied by means of sensitivity analyses of both the GM and MGM.

Study area description

The Kharga Oasis is one of the depressions located in the New Valley region in the southern part of the western desert of Egypt (Fig. 1). This oasis is bounded by the Eocene limestone plateau to the east and north, where steep cliffs form a sharp boundary. This limestone plateau stretches along the Middle and Upper Egypt at an elevation up to 550 m above mean sea level (amsl) (approximately 400 m above the depression floor of the oasis). The studied area lies between the latitudes 23°55′ to 26°N and the longitudes 30°7′ to 30°45′E, as shown in Fig. 1. The calculated area shown in Fig. 1 is used in the numerical analysis, as explained later.

The Kharga Oasis is situated in the tropical arid climate zone. The Kharga Oasis is one of the driest areas of the Eastern Sahara, which makes it one of driest areas on Earth (Kehl and Bornkamm 1993). The average potential evaporation rate reaches approximately 18.4 mm/day, and the mean annual value of relative humidity is approximately 39 %. The annual precipitation is extremely low and is almost insignificant (1 mm/year) (Salman et al. 2010).

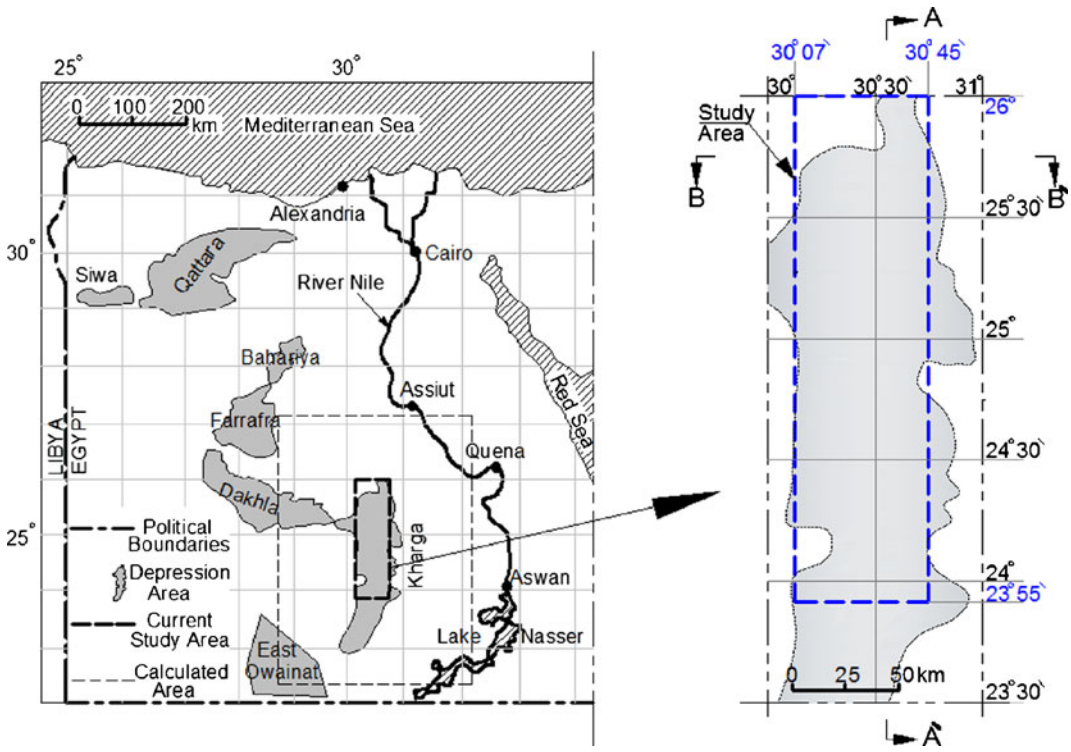

Fig. 1 Location map of the study area showing observed sites

The origin of groundwater in the NSAS has been extensively discussed by several authors since approximately 1920; two possibilities for the origin have been proposed. The older postulated concept is that the groundwater is supplied from precipitation in the southern mountainous parts of the NSAS. This concept was suggested primarily by Ball (1927) and supported by Sandford (1935). The newer postulate by Sonntag (1986) suggested that the bulk of the groundwater mass within the aquifer was originally supplied in situ during the humid pluvial periods (up to 30,000 years B.P.).

Lamoreaux et al. (1985) and Ebraheem et al. (2002) reported that the thickness of the Nubian Sandstone Aquifer beneath the Kharga Oasis ranged from 300 to 1,000 m. Lamoreaux et al. (1985) mentioned that the NSAS consists of thick sequences of coarse clastic sediments of sandstone and sandy clay embedded with shale and clay deposits. These impermeable clayey beds restrict the vertical movement of water between water-bearing layers. These beds of lower permeability, however, are lenticular and discontinuous; thus, regionally, the Nubian Sandstone forms a single aquifer complex. At the Kharga Oasis, Lamoreaux et al. (1985) classified these water-bearing layers of an average thickness of approximately 700 m into four layers. In the current study following Lamoreaux et al. (1985), the classification and the average thickness of each layer are defined as follows: (1) layer A, with an average thickness of 100 m (top layer); (2) layer B, with an average thickness of 235 m; (3) layer C, with an average thickness of 266 m, and (4) layer D, with an average thickness of 110 m (bottom layer). On the basis of this classification, layer A refers to the shallow aquifer, while the others (layers B, C, and D) refer to the deep aquifer.

Lamoreaux et al. (1985) reported that the extraction of groundwater was fairly stable from 1941 to 1953 and that a large proportion of the water was extracted from the shallow aquifer, most of the wells were artesian, and the change in the groundwater table was insignificant. Groundwater withdrawal from deeper layers started in 1960 to provide water supplies for proposed large-scale irrigated agriculture and new settlements at Kharga Oasis and to avoid over-exploitation of the shallow aquifer horizon which was previously the only source of water. Figure 2 shows the annual groundwater withdrawal in the study area in the period 1960–2009 from all of the shallow wells, all of the deep wells, and the total discharge as a sum of the deep and shallow well discharges.

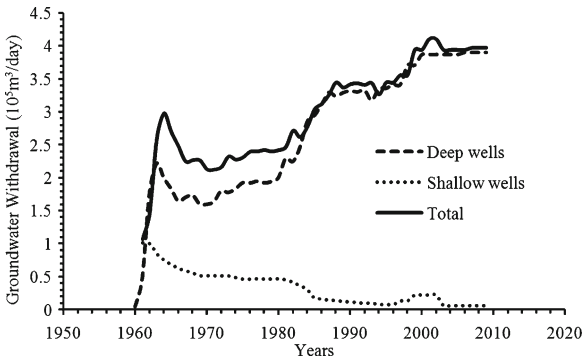

Fig. 2 History of groundwater withdrawal from deep and shallow aquifers

From this figure, it can be concluded that the discharge from the shallow wells has had an insignificant effect on the total discharge since 1983, while the discharge from the deep aquifers has increased significantly since 1962. The Food and Agriculture Organization (FAO) 1977 report noted that the decline in discharge from shallow wells may be due to the increase of production by deep wells, causing the hydraulic head to drop in the shallow aquifer. Consequently, production from the shallow wells can be neglected and is not included in the current study. Ball (1927), Sandford (1935), and Lamoreaux et al. (1985) noted that the general flow direction in the NSAS is from the southwest to the northeast. Heinl and Thorweihe (1993) estimated that the flow velocity in the deep aquifer is approximately 1 m/year, which means the groundwater would require over 100,000 years crossing the distance from either tropical infiltration area or the River Nile to reach the Kharga Oasis part of the NSAS. Ebraheem et al. (2003) reported that the permissible and economical lifting depth for the Kharga Oasis is 38 m below the ground surface.

Two types of wells are considered in this study, recent working production wells (RWPWs) and observation wells (OWs). Mahmod et al. (2013) divided the whole area into northern and southern parts and subdivided the studied area into eight subdivisions based on the distribution of settlements and RWPW allocations, as shown in Fig. 3. Mahmod et al. (2013) revealed that the middle area of the northern part (area 3–area 5) and area 7 in the southern part have the highest concentrations of RWPWs and were named the M region and the SN region, respectively.

Shata (1982) reported that the transmissivity and storage coefficient values for the NSAS under the Kharga Oasis were in the range of 100 to 2,000 m^2/day and 1.5×10^{-4} to 1.5×10^{-2}, respectively. Hesse et al. (1987) reported that the hydraulic conductivity of the Kharga part of the NSAS has an average value of 2.16 m/day. Ebraheem et al. (2002) noted that the average hydraulic conductivity for the regional NSAS is in the range of 0.0864 to 0.864 m/day, with an average storage coefficient of 1.0×10^{-4}. However, these hydraulic properties have not been confirmed for the entire aquifer.

Methodology

MGM concept

In the current study, the MGM was newly developed for the analysis of groundwater flow. Broadly speaking, the main concept of the MGM is quite similar to the GM because it combines a numerical model (NM) with a soft computing technique (SCT). Although the

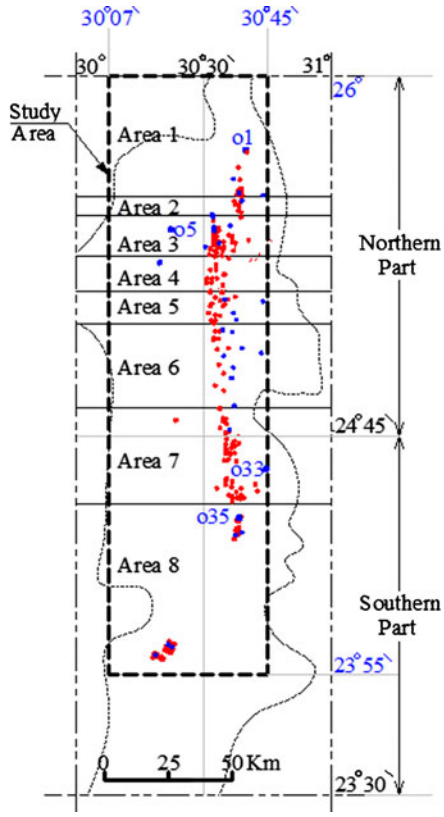

Fig. 3 Distribution of RWPWs and OWs over the Kharga Oasis. RWPWs are shown in *red* and OWs in *blue* (Mahmod et al. 2013). *Dotted line* indicates the schematic boundary of the Kharga Oasis. *Dashed line* indicates the current study area

GM has been proposed by some hydrogeologists (Mohammed et al. 2010; Mahmod et al. 2013), it has not yet been widely applied to groundwater problems. Mohammed et al. (2010) proposed a GM as a combination of a 3D-FEM with an artificial neural network (ANN) as the NM and SCT, respectively, with the aim of predicting the piezometric level change in the fractured rock mass at the Mizunami Underground Research Laboratory (MIU) in Japan. On the other hand, Mahmod et al. (2013) proposed a GM as a combination of a 2D-FEM with GAs to analyze groundwater flow in the Kharga Oasis. FEM was used to analyze groundwater flow under the assumption of hydrogeological and boundary conditions to produce approximate solutions for temporal piezometric level changes. Then, the GA model was used to fit the measured temporal piezometric level changes using these approximate solutions as inputs. In the GM, the number of input models' trends and the values of the input parameters are selected hypothetically before obtaining the best fitting values. The main problem in the GM is that there is no clear concept in the GA model for the selection of either the number of input models' trends or the values of input parameters, such as Population Size, Crossover Probability, Mutation Probability, and Number of Generations (fitting calculation time). For this purpose, a modification of the GA model was developed to omit the models which cause noise of fitting. The omitted models cause uncertainty of fitting because they have either a wide range of hydrogeological properties or calculation errors. As a result, the developed model can facilitate the selection of GA input parameters and consequently decreases the uncertainty of fitting to observations. Then, the effects of the best selected models' trends on the values of GA input parameters were studied. The GA model after modification will be called the Modified Genetic Algorithm (MGA) model. The combination of the best models' trends will be called the Best Models Combination (BMC_k), where *xk* is the number of selected models' trends). The MGM is the combination of FEM and MGA. As an application for MGM, this model is used to evaluate three different future exploitation/development plans under consideration for the aquifer system to explore the hydrological feasibility of these plans. The MGM simulation is applied for the period from the year 1960 to the year 2100.

The governing equation for two-dimensional saturated groundwater flow can be obtained by combining a special form of Darcy's law (derived from the water phase momentum balance) and the continuity equation written for the water phase (Anderson and Woessener 1992; Pinder and Gray 1977), as given in Eq. 1:

$$\frac{\partial}{\partial x}\left(T_{xx}\left(\frac{\partial}{\partial x}\right)\right)+\frac{\partial}{\partial y}\left(T_{yy}\left(\frac{\partial}{\partial y}\right)\right)=S\left(\frac{\partial h}{\partial t}\right)-W, \tag{1}$$

where T_{xx} and T_{yy} are the transmissivities along the x and y directions, respectively, h is the hydraulic head, S is the storativity, W is the groundwater volume flux per unit area (positive for outflow and negative for inflow), x and y are the Cartesian coordinates, and t is the time. As mentioned above, it is assumed from the geological consideration that the transmissivities and storativities are homogeneously distributed.

The FEM calculations were carried out assuming n different 2D hydrogeological models. For each model, the grid geometry and number of elements were identical. However, different sets of hydrogeological conditions, such as horizontal transmissivity in the x and y directions (T_{xx} and T_{yy}) and specific storage and boundary conditions, were assumed for each model. Then, n piezometric level trends ($H_1(t)$, $H_2(t)$,…, $H_n(t)$) were calculated by FEM. These simulated piezometric level trends were not representative of the measured piezometric level trends. The linear model (GA model) was used to reconstruct the measured piezometric level trend by combining the calculated piezometric level trends ($H_1(t)$, $H_2(t)$,…, $H_n(t)$), as given in Eq. 2 (Mahmod et al. 2013). For MGA, only the best models' trends were selected to be combined together by the Best Models Combination ($BMC_k(R_1(t)$, $R_2(t)$,…, $R_k(t)$, where R_k is the selected models' trends from H_n models' trends) to match the target measured trend (see Eq. 3):

$$H_s(t)=\sum_{i=1}^{n}\alpha_i\cdot H_i(t),\ \sum\alpha_i=1 \tag{2}$$

$$R_s(t)=\sum_{j=1}^{k}\alpha_j\cdot R_j(t),\ \sum\alpha_j=1,\ k\leq n, \tag{3}$$

where $H_s(t)$ and $R_s(t)$ are the reconstructed piezometric level trends at a certain location estimated by MG and MGM, respectively, $H_i(t)$ and $R_j(t)$ are the 2D-FEM simulated piezometric level trends, and α_i and α_j are the weight parameters. The produced weight parameters

can also be used for the future prediction of temporal piezometric level changes at any time (t). The structure of the MGM is schematically illustrated in Fig. 4.

Setting the hydrogeological model

Based on the hydrogeological properties of the Kharga Oasis part of the NSAS reported by previous researchers, n hydrogeological models were constructed. For each model, the transmissivity (T_{xx} and T_{yy}) and storativity values were assumed to be in the average ranges of 50 to 500 m^2/day and 3.28×10^{-3} to 3.28×10^{-2}, respectively. The NSAS in the Kharga Oasis area is only a small part of the entire NSAS in Egypt. Groundwater flow in the NSAS is governed by the conditions at the boundaries of the regional system. These conditions are not well defined for the Kharga Oasis area. Because of this lack of clarity, the boundary condition was assumed as a fixed boundary head with the flow direction from the southwest to the northeast. With that assumption, the boundary conditions were expressed as the hydraulic head values given at the four corners (Z1–Z4) of the calculated area indicated in Fig. 1. Hydraulic heads along each boundary line were assumed to change linearly, as shown in Fig. 5. The values of Z1, Z2, Z3, and Z4 were roughly estimated by considering the goodness of fit between the calculated and measured piezometric level trends. In this study, 16 hydrogeological models were assumed with different sets of hydrogeological and boundary conditions, as summarized in Table 1.

To reduce the direct effects of boundary conditions on the results, the calculated area was extended beyond the study area boundary, as shown in Fig. 1. This area was subdivided into 24,069 rectangular elements and 24,396 nodes with the RWPWs and OWs located on the mesh nodes. The elements around the RWPWs and OWs were set as the smallest elements with the sizes gradually increasing toward the boundary of the calculated area, as illustrated in Fig. 5. The minimum and maximum lengths of the element sides were 377 and 7,000 m, respectively.

Proposed future scenarios for groundwater withdrawal

Although the total discharge extracted from the Kharga Oasis part of the NSAS is known from 1960 to 2009 (Fig. 3), the discharge for each production well in the same period is unknown. For this reason, a scenario of groundwater withdrawal of each RWPW was assumed to follow the same groundwater withdrawal trend as the total discharge curve given in Fig. 3, considering that the discharge was almost steady within the period 2005–2009. From 2009 to the present, groundwater withdrawal was assumed to continue being steady. Hereafter, for each RWPW, three scenarios of groundwater withdrawal are assumed, considering that no new production wells will be constructed. The main criterion in the three proposed scenarios is to keep the

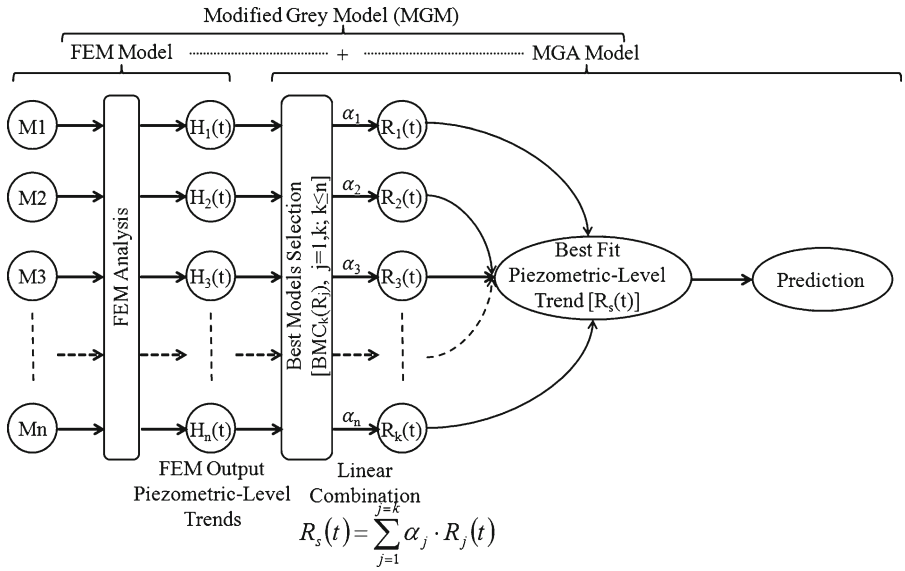

Fig. 4 Structure of the developed Modified Grey Model (MGM)

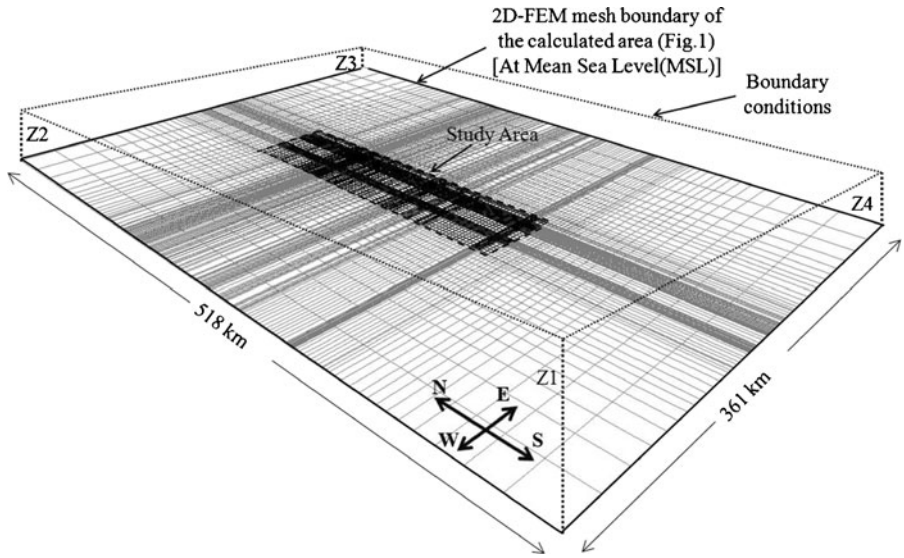

Fig. 5 Adopted 2D-FEM mesh geometry for the calculated area and the study area. Z1–Z4 are the assumed hydraulic heads at the corners of the calculated area

sum of groundwater withdrawal from the current study area constant. These scenarios are explained as follows:

Scenario 1 The present groundwater withdrawal is increasing and kept constant until the final simulation year of 2100.

Scenario 2 In this scenario, the groundwater withdrawal is redistributed among the RWPWs in the M region and the southern subdivision area 8. Area 8 is the highest piezometric level area of the study area (Lamoreaux et al. 1985; Mahmod et al. 2013). In this scenario,

Table 1 Proposed hydrogeological models

Model name	Corner hydraulic heads				T_{xx} (m/day)	T_{yy} (m/day)	S ($\times 10^{-3}$)
	Z1 (m)	Z2 (m)	Z3 (m)	Z4 (m)			
M1	87	220	150	105	50	50	32.8
M2	37	170	100	55	50	50	3.28
M3	27	160	90	45	50	500	3.28
M4	37	170	100	55	5	50	3.28
M5	37	170	100	55	500	500	32.8
M6	85	85	85	85	50	500	3.28
M7	37	170	100	100	50	500	3.28
M8	−282	484	123	−111	50	500	3.28
M9	−282	484	123	−90	50	500	3.28
M10	−282	490	123	−111	50	500	3.28
M11	−300	484	123	−111	50	500	3.28
M12	−297	495	108	−126	50	500	3.28
M13	−282	484	123	−111	138	500	3.28
M14	−282	484	123	−111	50	50	3.28
M15	−232	534	123	−61	97	500	3.28
M16	−282	484	123	−111	138	500	32.8

the groundwater withdrawal in the M region is equal to that in the first scenario reduced by 20 %. Then, the sum of the groundwater withdrawal reduced from the RWPWs of the M region is distributed over the RWPWs in area 8 while keeping the ratio between the RWPW discharges constant (see Eqs. 4 and 5).

$$\sum Q_{\mathrm{M\ region}} = 0.80 \times \sum Q_{\mathrm{M\ region(Scenario\ 1)}} \quad (4)$$

$$\sum Q_{Area\ 7} = \sum Q_{Area\ 8(Scenario\ 1)} + 0.20 \times \sum Q_{\mathrm{M\ region(Scenario\ 1)}} \quad (5)$$

Scenario 3 In this scenario, groundwater withdrawal is redistributed among the RWPWs in the northern part and the southern subdivision area 8. The groundwater withdrawal of the northern part of this scenario is equal to that in the first scenario reduced by 5 %. Then, the sum of the groundwater withdrawal reduced from the RWPWs in the northern part is distributed among the RWPWs in area 8 while keeping the ratio between the RWPW discharges constant (see Eqs. 6 and 7):

$$\sum Q_{Northern\ part} = 0.95 \times \sum Q_{Northern\ part(Scenario\ 1)} \quad (6)$$

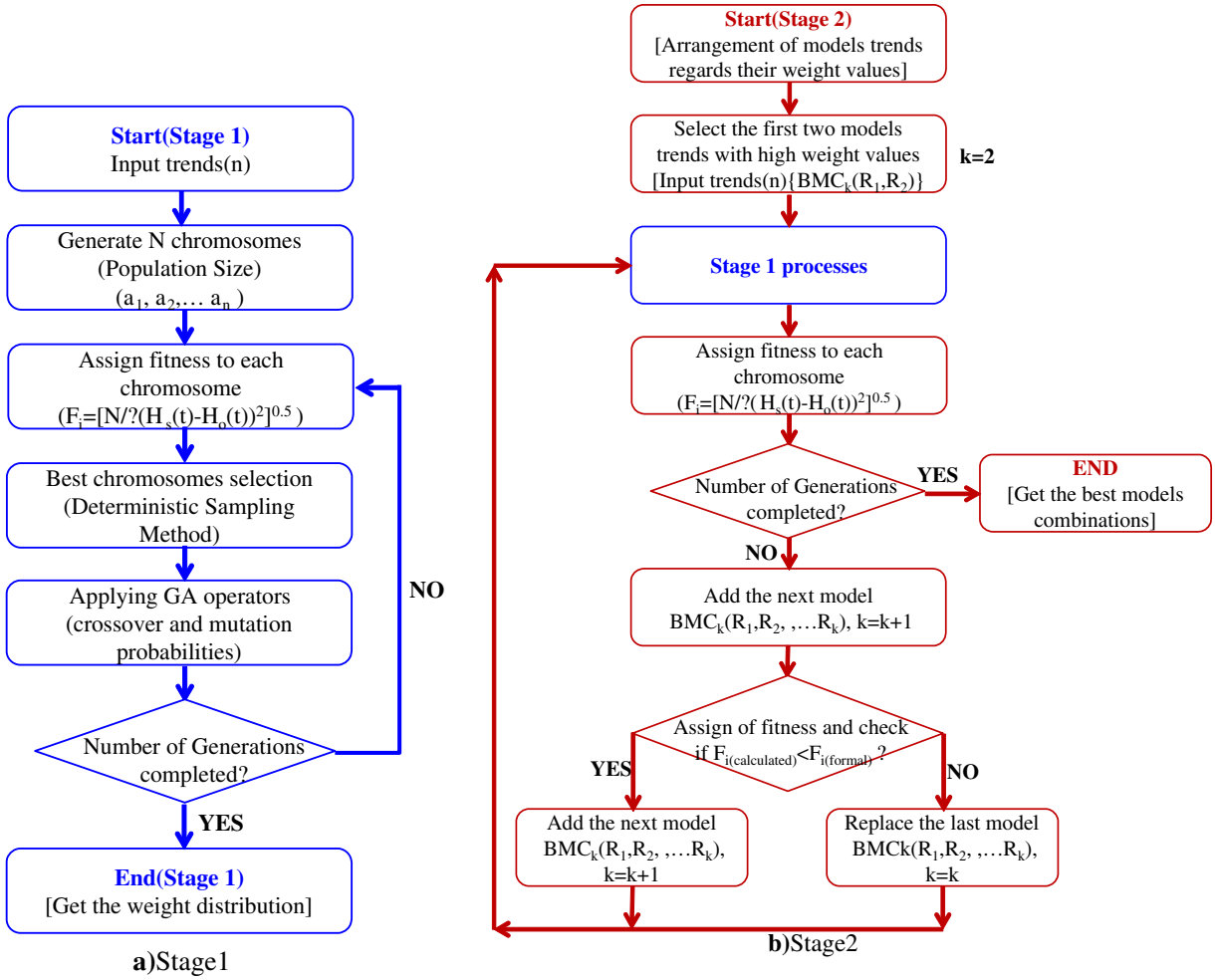

Fig. 6 Flow chart describing the MGA optimization process: **a** stage 1 and **b** stage 2

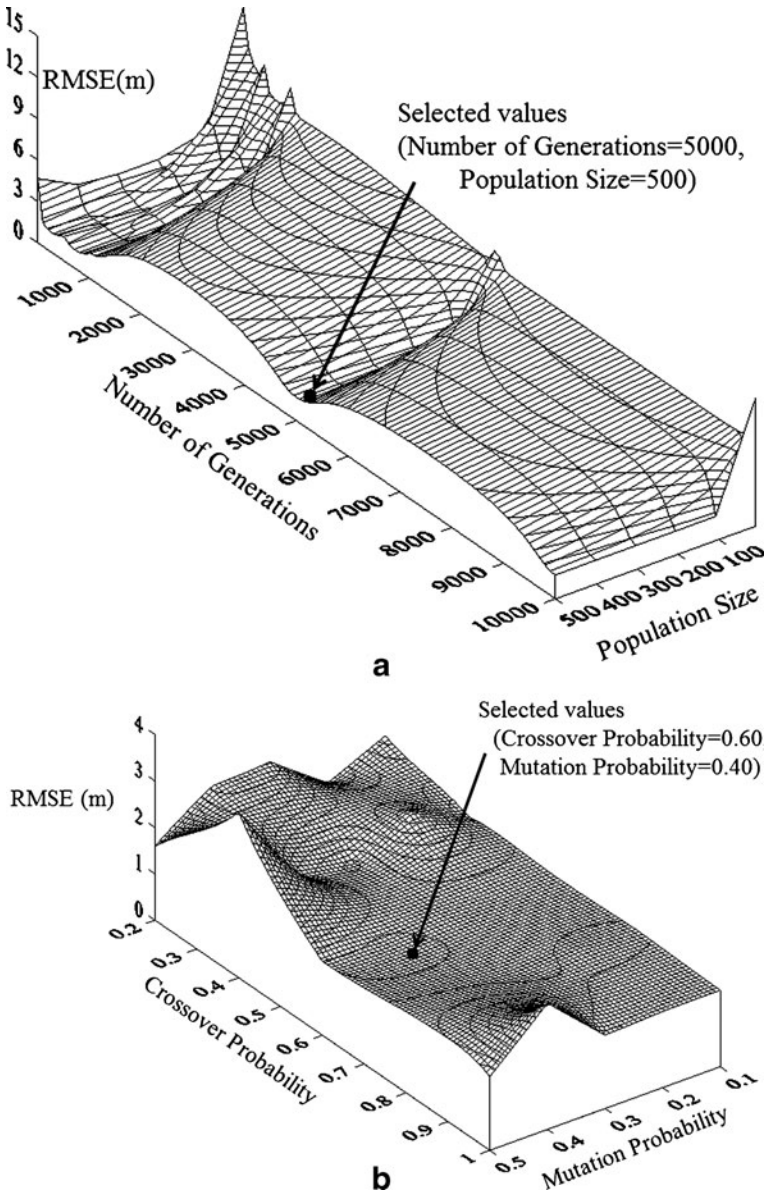

Fig. 7 Sensitivity range analysis for the GM: **a** Number of Generations and Population Size and **b** Crossover and Mutation Probabilities

$$\sum Q_{Area\ 7} = \sum Q_{Area\ 8(Scenario\ 1)} + 0.05 \times \sum Q_{\mathrm{M}\ region(Scenario\ 1)}, \quad (7)$$

for which Q is the groundwater withdrawal of each RWPW.

Setting the MGA model

Many researchers reported that the GA model provides good performance for estimating the optimum combination of weight parameters (Watanabe et al. 2012; Mahmod et al. 2013). This combination of weight parameters is called a chromosome ($\alpha_1, \alpha_2, \ldots, \alpha_n$), and each weight parameter is called a gene. However, the optimum number of inputs (hydrogeological models) and the values of the input parameters remain a problem. For this reason, the GA model has been modified by adding a selection process for finding the optimum input models' trends. This newly developed model is called the MGA. The selection process is used for selecting the best inputs that achieve an appropriate goodness of fit with the measured piezometric level trends. The number of selected

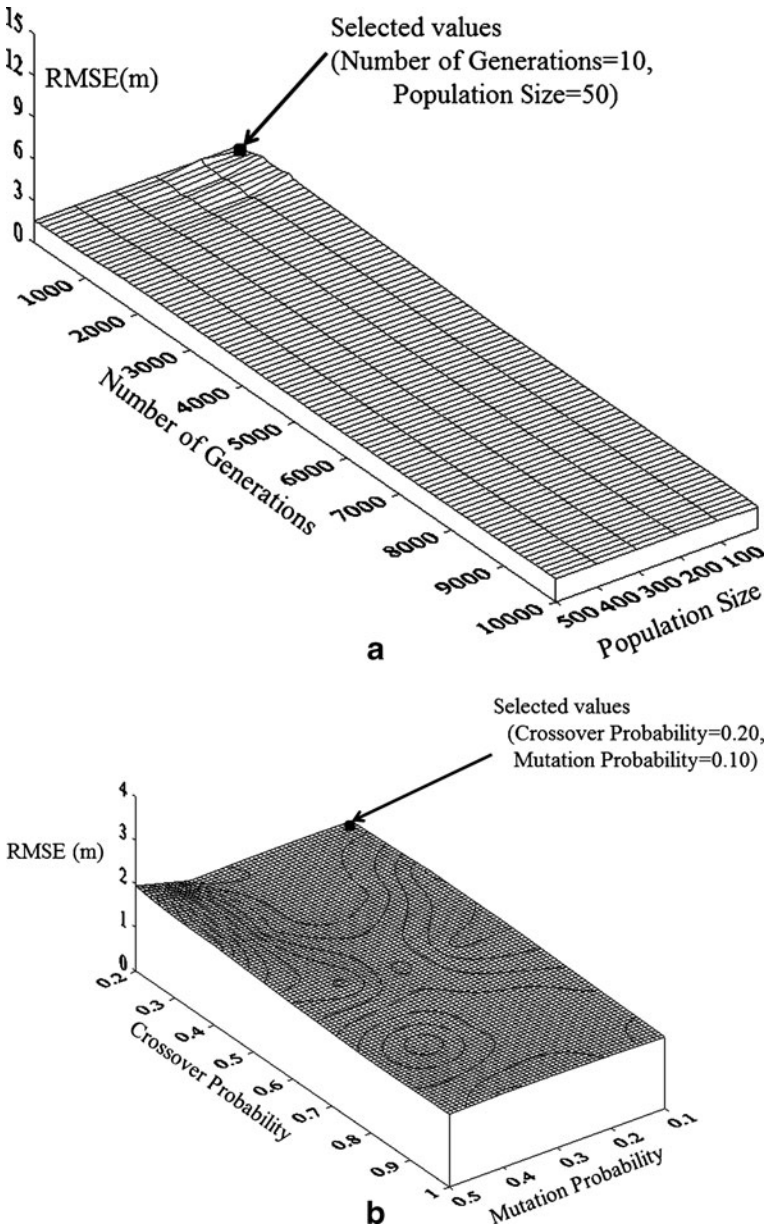

Fig. 8 Sensitivity range analysis for the MGM: **a** Number of Generations and Population Size and **b** Crossover and Mutation Probabilities

inputs is "*k*," and the combination of these inputs is called the BMC_k. The concept of the proposed model (MGA) could be described in two stages as follows:

Stage 1 (preliminary weight distribution): The process in this stage is the same as in the ordinary GA model (Mahmod et al. 2013); however, the target of this stage is not determining the optimum weight parameters. This stage is used to obtain a preliminary weight distribution for the inputs with any value for the Number of Generations. For this reason, using a small Number of Generations is enough to obtain this type of distribution. This stage contains the following main steps (see Fig. 6a):

1. After simulating groundwater flow using the hydrogeological model explained previously, *n* temporal trends of hydraulic heads ($H_1(t)$,

Table 2 Setting of GA and MGA model parameters

Parameters	For minimum RMSE		Selected parameters	
	GA	MGA	GA	MGA
Number of Generations	5,000	10–10,000	5,000	10
Population Size	≥100	10–500	500	50
Crossover Probability	0.60–0.70	0.2–1.0	0.60	0.20
Mutation Probability	≥0.35	0.1–0.4	0.40	0.10

$H_2(t),\ldots, H_n(t)$) are obtained and used as inputs to the GA model. Then, N different chromosomes are generated by giving random values in the range of 0.0–1.0 as genes. The gene values are adjusted to fit the criterion that the sum of the genes in each chromosome should equal to 1.0. The number of chromosomes N is called the Population Size.

2. Equation 2 is applied to obtain the reconstructed piezometric level trend ($H_s(t)$). Then, the fitness values (F_i) between the measured ($H_o(t)$) and the reconstructed piezometric level trends ($H_s(t)$) for every chromosome are calculated (see Eq. 8).

$$F_i = \sqrt{\frac{N}{\sum_{i=1}^{i=N}\left(H_S(t)-H_o(t)\right)^2}} = \frac{1}{RMSE}. \qquad (8)$$

3. The best-fit chromosomes are selected using a deterministic sampling method (Sivaraj 2011; Goldberg and Deb 1991). In this method, the average fit of the population is calculated. Then, the fitness for each chromosome is divided by the average fitness, but only the integer part of this operation is used to select individuals. Then, the entire fraction is used to sort the individuals. The remaining free places in the new population are filled with the chromosomes that have the largest fraction values in the sorted list.
4. T hese "n" models' trends are processed by GA processes (crossover and mutation processes) to obtain the final weight parameters (α_1, α_2,…, α_n) that are used in Eq. 2. At the initial stage, the weight parameters are given as random numbers. Then, the weight parameters are pursued through the repetition of cross-over and mutation processes (Coley 1999) until completing the selected Number of Generations. Cross-over and mutation processes are represented by two operators: Crossover Probability and Mutation Probability (Mitchell 1999).

Stage 2 (obtaining the $BMC_k(R_j(t))$; j=1, k; $k \leq n$): Regarding stage 1, the weights of each input for fitting the observed trend were recognized. In this stage, the inputs are renamed according to

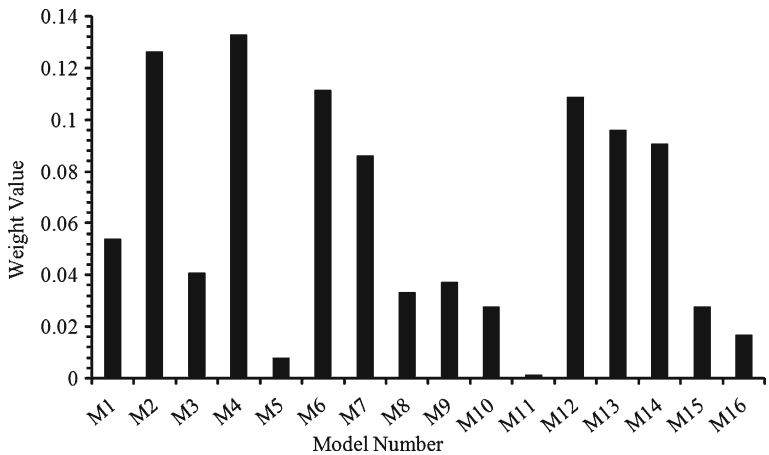

Fig. 9 Preliminary weight distribution of the hydrogeological models

Table 3 Combinations of hydrogeological models' trends

Combination no.	Combined models' trends
1	M4, M2
2	M4, M2, M6
3	M4, M2, M6, M12
4	M4, M2, M6, M12, M13
5	M4, M2, M6, M12, M13, M14
6	M4, M2, M6, M12, M13, M14, M7
7	M4, M2, M6, M12, M13, M14, M7, M1
8	M4, M2, M6, M12, M13, M14, M7, M1, M3
9	M4, M2, M6, M12, M13, M14, M7, M1, M3, M9
10	M4, M2, M6, M12, M13, M14, M7, M1, M3, M9, M8
11	M4, M2, M6, M12, M13, M14, M7, M1, M3, M9, M8, M15
12	M4, M2, M6, M12, M13, M14, M7, M1, M3, M9, M8, M15, M10
13	M4, M2, M6, M12, M13, M14, M7, M1, M3, M9, M8, M15, M10, M16
14	M4, M2, M6, M12, M13, M14, M7, M1, M3, M9, M8, M15, M10, M16, M5
15	M4, M2, M6, M12, M13, M14, M7, M1, M3, M9, M8, M15, M10, M16, M5, M11

their weights from $R_1(t)$ for the highest weight input to $R_n(t)$ for the lowest weight input. Hereafter, the following steps take place (see Fig. 6b):

1. The first two inputs ($BMC_k(R_j(t))$; j=1, k; k=2) are combined using the GA model (stage 1 procedures). Then, $R_s(t)$ is calculated (Eq. 3), and the fitness with the observed trend $R_o(t)$ is calculated using Eq. 8.
2. The third input $R_3(t)$ is added to the formal combination to become $BMC_3(R_1(t), R_2(t), R_3(t))$ and then the fit is recalculated.
3. If the calculated fit is less than the formal fit ($F_{calculated}<F_{formal}$), then the input will be added to the combination to become $BMC_4(R_1(t), R_2(t), R_3(t), R_4(t))$. On the contrary, if the calculated fit is larger than the formal fit, the last input in the combination $BMC_3(R_1(t), R_2(t), R_3(t))$ will be replaced by its next input to become $BMC_3(R_1(t), R_2(t), R_4(t))$. This process is continued until the selected Number of Generations has been completed.
4. The Best Models Combination ($BMC_k((R_1(t), R_2(t),\ldots, R_k(t))$ is obtained.

The two stages explained above are applied on a part of the time series data as training for the model (training phase). The other part of the data is used for the validation of the resulting weights

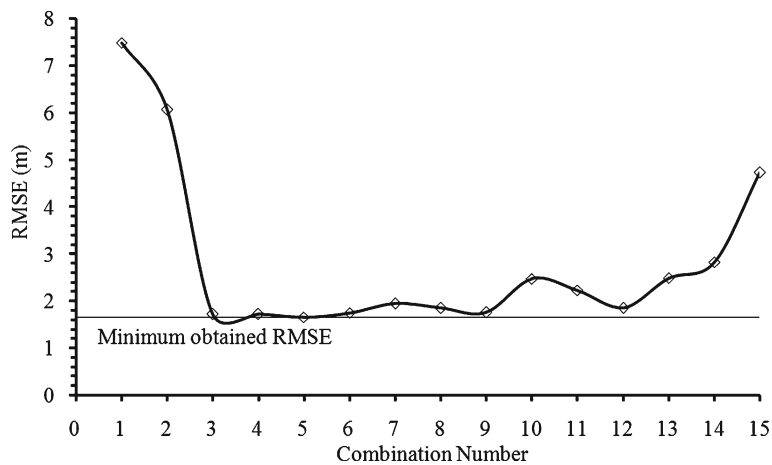

Fig. 10 Effect of the number of inputs on the performance of the ordinary GA model

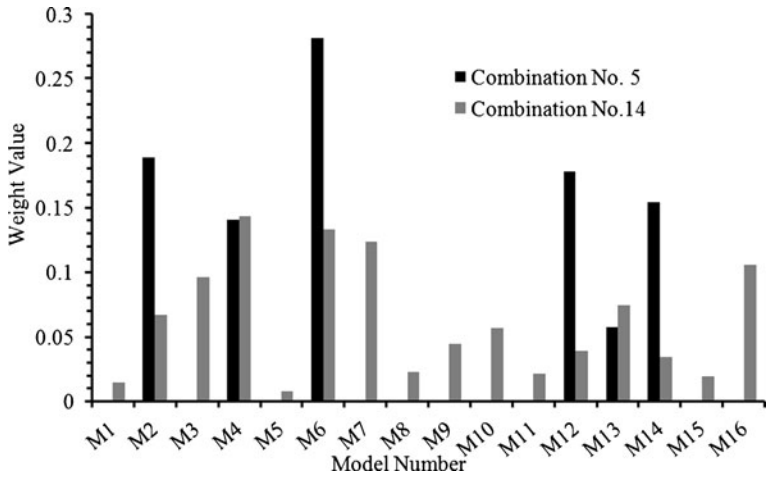

Fig. 11 Weight distribution for combination numbers 5 and 15

(test phase). Due to the limited data and to guarantee good results at the prediction phase and in future assessment, a large percentage of the data is used in the training phase, and the other remains for the prediction phase.

Results and discussion

Sensitivity analysis

The input parameters including Population Size, Crossover Probability, Mutation Probability, and Number of Generations should be properly pre-determinate for the MGA model analysis. Moreover, the comparison between the goodness of fit of the MGA and GA models should be analyzed under the different values of the input parameters. For this purpose, a sensitivity analysis is carried out to properly select the appropriate values of these parameters. In the present analysis, the measured piezometric level trend for observation well (OW) o1 is used as a target. The relationships among root mean square error (RMSE), Number of Generations, and Population Size is shown in Fig. 7a while the relationship among RMSE, Crossover Probability, and Mutation Probability is shown in Fig. 7b. Similarly, for MGA model, the relationships among RMSE, Number of Generations, and Population Size is shown in Fig. 8a, and that among RMSE, Crossover Probability, and Mutation Probability is shown in Fig. 8b. It can be noticed from Fig. 7a that the minimum value of the RMSE is attained at a Number of Generations of 5,000 and a Population Size that is greater than 100. However, the relationships among RMSE, Crossover Probability, and Mutation Probability are more complicated as shown in Fig. 7b. Figure 7b shows that the smallest value of RMSE is attained at a Crossover Probability value between 0.6 and 0.7 and a Mutation Probability that is larger than 0.35. On the contrary, Fig. 8a, b shows highly stable and smooth relationships over a wide range of parameter values. Based on these results, the selected

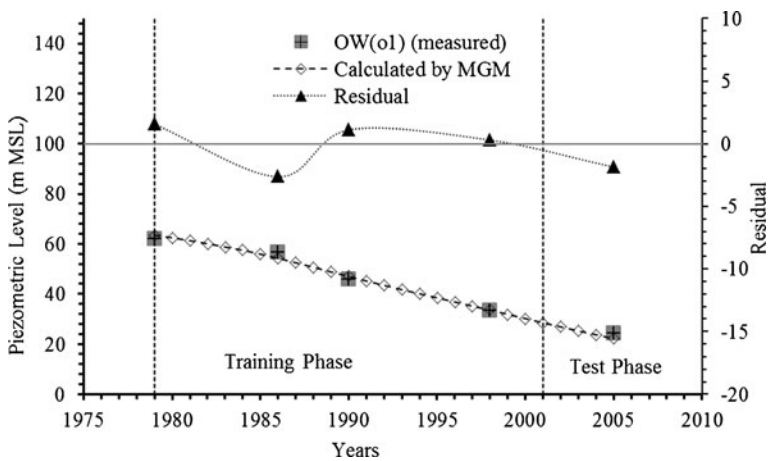

Fig. 12 Comparison of MGM-calculated and measured piezometric level values of OW o1 for training and test phases

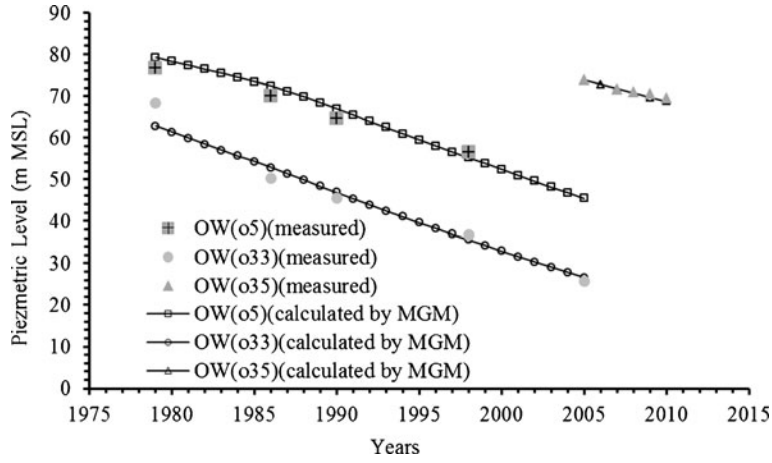

Fig. 13 MGM-calculated piezometric level trends for OWs o5, o33, and o35

values of the input parameters for the GA and MGA models are summarized in Table 2. Consequently, MGA produces a goodness of fit between measured and calculated piezometric levels over a wide range of input parameter values.

Effect of input models' trends on ordinary GA performance

As a result of the previous sensitivity analysis for the ordinary GA model, stable relationships are attained only at a narrow range of the input parameters. Moreover, the relationships among RMSE and the input parameters are complicated and noisy until the minimum RMSE is achieved. Hence, it is highly important to find the reason behind this noise to increase the stability of the ordinary GA model. The preliminary weight distribution produced at the first stage of the MGA model explained previously is shown in Fig. 9. This type of distribution is obtained by assuming the values of the input parameters including Population Size, Crossover Probability, Mutation Probability, and Number of Generations as 50, 0.2, 0.1, and 10, respectively. As a first step to check the performance of fit for the GA model and considering the weight values shown in Fig. 9, the models' trends can be arranged from the highest weight value to the lowest one. Then, the input models' trends are progressively combined together using the GA model, and the resulting combinations are illustrated in Table 3. For the target observation OW o1, RMSE is obtained as a measurement of fit for every combination, as shown in Fig. 10. It can be noticed from this figure that using a large number of input models' trends causes an increase in RMSE value, which reflects instability in the fit performance. As a way to explain the reason for this instability, the weight distribution of these combinations should be analyzed. The lowest value of RMSE is associated with combination no. 5, while the highest one is obtained with combination no. 15. Figure 11 shows the weight distribution of the combination nos. 5 and 15 which indicates a high variation in the weight distribution between the two combinations. For example, the M6 trend has the highest weight value at combination no.

Table 4 The Best Models Combination (BMC_k) selected by the MGM for the target OWs

OW name	$BMC_k(R_j(t))$; j=1, k; $k \leq n$	% reduction of input
o1	BMC_4(M4, M2, M6, M12)	75
o5	BMC_5(M2, M3, M6, M12, M5)	68.75
o33	BMC_4(M11, M9, M2, M15)	75
o35	BMC_3(M5, M10, M1)	81.25

Table 5 CE, CD, and RMSE obtained for the target OWs for the MGM and GM

OW name	MGM			GM		
	CE	CD	RMSE	CE	CD	RMSE
o1	0.985	0.994	1.738	0.986	0.994	1.678
o5	0.914	0.995	2.164	0.981	0.996	1.013
o33	0.957	0.983	2.936	0.965	0.986	2.665
o35	0.966	0.985	0.630	0.985	0.999	0.439

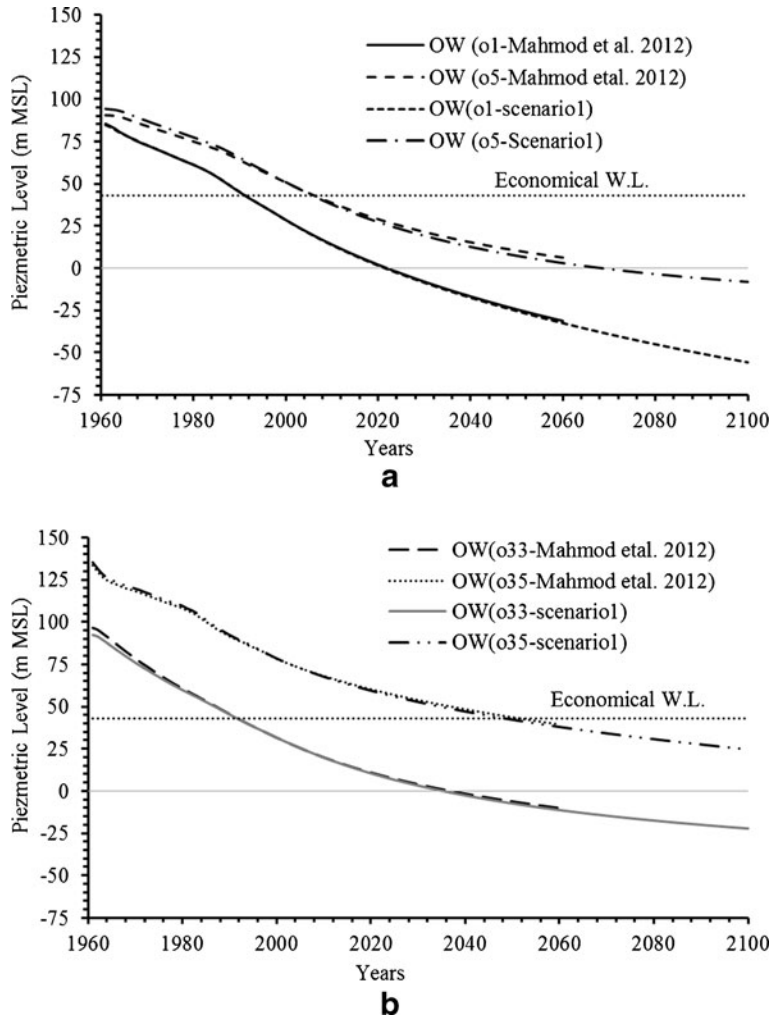

Fig. 14 Comparison of simulated piezometric levels for MGM and GM (Mahmod et al. 2013) until the year 2100: **a** OWs o1 and o5 and **b** OWs o33 and o35

5; however, the trend of M4 has the highest weight value at combination no. 15. Consequently, using the GA model, some considerations are difficult to properly achieved, such as stability and convergence; this may be attributed to the variation of models' weight values from one combination to another.

MGM results

The result of the MGM analysis for OW o1 as a representative of area 1 is shown in Fig. 12 at which the residual error between the calculated and measured piezometric level values is plotted. Figure 13 shows the MGM-simulated piezometric level trends for OWs o5, o33, and o35 as targets and representatives for the M region, SN region, and area 8, respectively (see Fig. 2). Also, the best input models' trends (BMC_k) used for the best fit with the measured piezometric level trends of the target OWs are illustrated in Table 4. This table indicates that the number of input models' trends used by the GM (n=16 models' trends) is reduced when using the MGM, and the percentage of reduction is calculated using Eq. 9. This percentage illustrates a high reduction in the number of input models' trends for the MGM in the range between 68.75 and 81.25 %, which is a considerably high percentage.

$$\%reduction = \frac{n-k}{n} \times 100. \quad (9)$$

Three statistical quantities were used to assess the performance and accuracy of the MGM: the coefficient of efficiency (CE), the coefficient of determination (CD), and the root mean square error. With such limited amount of data, it is not appropriate to calculate these coefficients separately for the training phase and the test phase. Hence, these coefficients are calculated for both phases together. For a perfect prediction, the CD and the

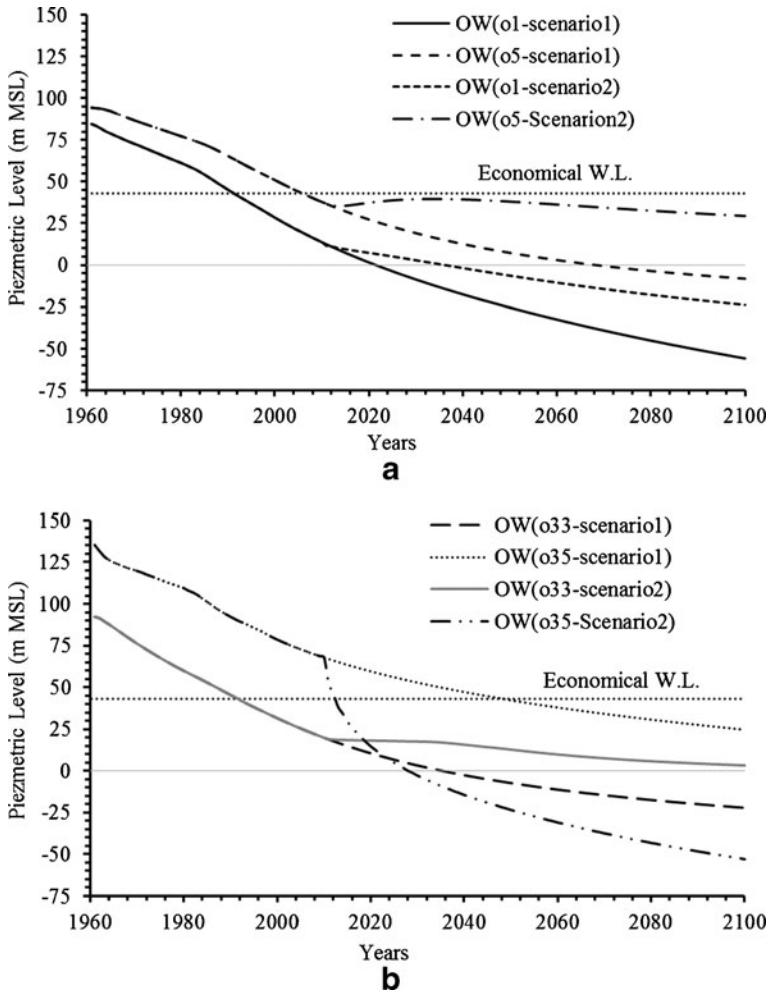

Fig. 15 Comparison of MGM-simulated piezometric levels for scenario 2 and scenario 1 until the year 2100: **a** OWs o1 and o5 and **b** OWs o33 and o35

CE approach 1, while the RMSE approaches 0 (Spitz and Moreno 1996; Nash and Sutcliffe 1970). Shamseldin (1997) claimed that models having CE values above 0.9 are very satisfactory, those with values between 0.8 and 0.9 are fairly good, and those with values below 0.8 are unsatisfactory. The results in Table 5 indicate that the MGM has been calibrated successfully and that the values of CE, CD, and RMSE are satisfactory compared to those of the GM.

Assessment and evaluation of proposed groundwater development plans

The good agreement between the measured and calculated piezometric level trends in the short period simulation (1979–2005) was considered to be a verification of the MGM presented in this study. Thus, the MGM can be used to predict piezometric level trends and drawdown of the groundwater table over long periods as well as to evaluate the hydrological feasibility of the proposed groundwater withdrawal plans (scenarios 1, 2, and 3). Regarding the proposed scenarios for groundwater withdrawal described previously, the simulated declines in hydraulic head at the target OWs are calculated for the period of 1960 to 2100. The permissible and economical lifting depth for the Kharga Oasis area is 38 m below the ground surface (Ebraheem et al. 2003). Therefore, for the target OWs (i.e., o1, o5, o33, and o35), the average economical piezometric level is calculated as 43 m above the mean sea level.

For the proposed scenarios of groundwater withdrawal scenario 1, scenario 2, and scenario 3, the simulated piezometric levels of the target OWs are shown in Figs. 14, 15, and 16, respectively. Regarding scenario 1, Fig. 14 shows a comparison of piezometric level trends simulated by the MGM and those simulated by the GM

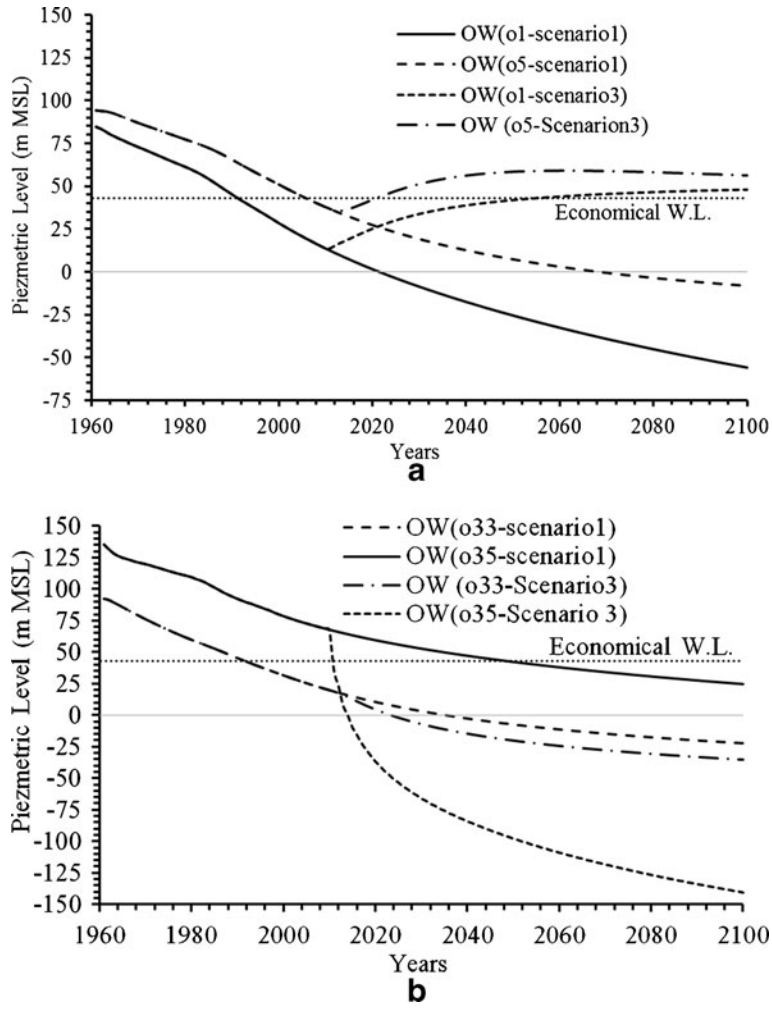

Fig. 16 Comparison of MGM-simulated piezometric levels for scenario 3 and scenario 1 until the year 2100: **a** OWs o1 and o5 and **b** OWs o33 and o35

(Mahmod et al. 2013) for the target OWs. The result from this comparison shows a high correlation between the MGM and GM trends which confirms the validity of the newly developed MGM for future assessment of hydraulic heads; however, the MGM input parameter values are smaller than those of GM. Also, the figure shows that the piezometric levels of the target OWs o1, o5, and o33 have already reached economical levels in 1995, 2009, and 1996, respectively, and are expected to decline during the simulation period, while the piezometric level OW o35 is expected to reach the economical level by the year 2060. Although the MGM use a small number of inputs and low values of the input parameters, the model introduces satisfactory valid results compared to the ordinary GM. Moreover, the time required for calculations, represented by the Number of Generations' parameter, is reduced from 5,000 for the GM to 10 for the MGM, which is a considerably a large reduction of 99.98 %.

For scenario 2, Fig. 15 shows that the hydraulic heads of OWs o1, o5, and o33 are recovered by 32.0, 37.5, and 25.0 m, respectively, compared to those in scenario 1.

Table 6 Hydraulic head differences in the economical piezometric levels for the target OWs

OW	Difference from the economical piezometric level (43 m) by 2100		
	Scenario 1	Scenario 2	Scenario 3
o1	−98.88	−66.89	4.98
o5	−51.16	−13.58	13.27
o33	−65.22	−39.76	−78.26
o35	−18.33	−96.08	−183.62

On the contrary, the hydraulic head of OW o35 is severely decreased by 77.8 m. Comparing scenario 3 with scenario 1, Fig. 16 shows that the hydraulic heads of OWs o1 and o5 are recovered by 104.0 and 64.5 m, respectively, to reach their economical piezometric levels by the years 2039 and 2018. On the other hand, the hydraulic heads of OWs o33 and o35 are decreased by 13 and 165 m, respectively. For both scenarios 2 and 3, the high decrease in hydraulic head of OW o35 as a representative of area 8 is due to the high groundwater withdrawal that added to the RWPWs in this area. Therefore, it is recommended that new production wells should be constructed in the southern part (area 8) far enough from the RWPWs to redistribute the groundwater withdrawal over these production wells. For the three scenarios, Table 6 shows the differences in hydraulic heads between the economical piezometric head levels and the target OWs' piezometric levels beyond 2100. A positive sign indicates that the piezometric level of the OW is above the economical one and vice versa.

As the best input models' trends in MGM are elected by means of the BMC_k, the MGM shows a better fitting performance than the ordinary GM. On the other hand, the MGM produces a wide range of input parameter values, which guarantees goodness of fit with any hypothetical value of these parameters.

Conclusions

Lack of hydrogeological data often limits the implementation of the numerical models which are used for analyzing the groundwater flow over a study area. In the current study, Kharga Oasis was used as a case study at which groundwater flow was analyzed using a newly developed MGM trying to overcome the lack of basic data. The MGM is a combination of FEM with a newly developed MGA model. The FEM was used to analyze groundwater flow under the assumption of hydrogeological and boundary conditions to produce approximate solutions for temporal piezometric level changes. The MGA model was used to fit the measured temporal piezometric level changes. The major advantage of the developed MGA model compared to the ordinary GA model is the new selection criterion for selecting the best input models' trends that achieve an appropriate goodness of fit by means of the BMC_k. The following remarks can be drawn from this study:

- The MGA produces a goodness of fit to the observations using a wide range of input parameter values, while the ordinary GA produces the same fit performance using a narrow range of input parameter values.
- For the MGA, the time required for calculations, represented by the value of Number of Generations' parameter, was reduced by 99.8 % compared to the GM.
- The ordinary GA produces unstable fit performance with the observed piezometric level in spite of using a large number of input models' trends.
- For achieving goodness of fit, the MGM uses a smaller number of input models' trends than the ordinary GM with a considerably high percentage of reduction ranges from 68.75 to 81.25 %.
- The MGM predictions from the various scenarios of groundwater withdrawal demonstrate that if the present extraction rate is expanded (scenario 1), the groundwater piezometric level will continuously decline and drop below the economical piezometric level until the end of the simulation period at year 2100.
- To avoid groundwater depletion in the Kharga Oasis, the extraction rate in the M region is lowered by 20 % and added to area 8 (scenario 2). The planned extraction rate is not feasible for the future and will have a negative impact on the piezometric level of area 8. However, a recovery in the piezometric levels for all other subdivisions was observed.
- For the third scenario of groundwater withdrawal, the recovery head for the northern area increased more than that in scenario 2 and exceeded the economical piezometric level. However, a large drawdown of the piezometric level of the southern part was observed.
- Regarding the proposed scenarios and to protect the groundwater table from being severely drawn down at the southern area (area 8), it is suggested that new production wells should be constructed far enough from the RWPWs in this area.

References

Anderson, M. P., & Woessener, W. W. (1992). *Applied groundwater modeling: simulation of flow and advective transport*. San Diego: Academic.

Ball J. (1927). Problems of the Libyan Desert. *Geographical Journal, 70*:21–38, 105–128, 209–224.

Coley, D. A. (1999). *An introduction to genetic algorithms for scientists and engineers*. Singapore: World Scientific.

Ebraheem, A. M., Riad, S., Wycisk, P., & Seif El Nasr, A. M. (2002). Simulation of impact of present and future groundwater extraction from the non-replenished Nubian Sandstone Aquifer in SW Egypt. *Environmental Geology, 43*, 188–196.

Ebraheem, A. M., Garamoon, H. K., Wycisk, P., & Seif El Nasr, A. M. (2003). Numerical modeling of groundwater resource management options in the East Oweinat area, SW Egypt. *Environmental Geology, 44*, 433–447.

Goldberg, D. E., & Deb, K. (1991). A comparative analysis of selection schemes used in genetic algorithms. In G. J. E. Rawlins (Ed.), *Foundations of Genetic Algorithms*. California: Morgan Kaufmann Publishers Inc.

Heinl M., Thorweihe U. (1993). Groundwater resources and management in SW Egypt. In B. Meissner, P. Wycisk (Eds.), *Geopotential and Ecology*. Catena Suppl, 26 (pp. 99–121). Reiskirchen: Catena

Hesse, K., Hissne, A., Kheir, O., Schnäcker, E., Schneider, M., & Thorweihe, U. (1987). Hydrogeological investigations in the Nubian Sandstone Aquifer System, Eastern Sahara. *Berliner Geowissenshaftliche Abhandlungen, A75*, 397–4641.

Kehl H., Bornkamm R. (1993). Landscape ecology and vegetation units of the Western Desert of Egypt. In B. Meissner, P. Wycisk (Eds.) *Geopotential Ecology: Analysis of a Desert Region*. Catena Suppl, 26 (pp. 155–178). Reiskirchen: Catena

Lamoreaux, P. E., Memon, B. A., & Idris, H. (1985). Groundwater development, Kharga Oasis, western desert of Egypt: a long-term environment concern. *Environmental Geology and Water Sciences, 7*, 129–149.

Mahmod, W. E., Watanabe, K., & Zahr-Eldeen, A. A. (2013). Analysis of groundwater flow in arid areas with limited hydrogeological data using Grey Model: a case study of the Nubian Sandstone, the Kharga Oasis, Egypt. *Hydrogeology Journal, 21*, 1021–1034.

Mitchell, M. (1999). *An Introduction to Genetic Algorithms, 5th printing*. London: Massachusetts Institute of Technology.

Mohammed, M., Watanabe, K., & Takeuchi, S. (2010). Grey model for prediction of pore pressure change. *Environmental Earth Science, 60*, 1523–1534.

Nash, J. E., & Sutcliffe, J. V. (1970). River flow forecasting through conceptual models. Part 1. A discussion of principles. *Hydrogeology Journal, 10*, 282–290.

Nour, S. (1996). Groundwater potential for irrigation in the east Oweinat area, Western Desert, Egypt. *Environmental Geology, 27*, 143–154.

Pinder, G. F., & Gray, W. G. (1977). *Finite Element Simulation in Surface and Subsurface Hydrology*. New York: Academic.

Salman, A. B., Howari, F. M., El-Sankary, M. M., Wali, A. M., & Saleh, M. M. (2010). Environmental impact and natural hazards on Kharga Oasis monumental sites, Western Desert of Egypt. *Journal of African Earth Sciences, 58*, 341–353.

Sanford, K. S. (1935). Source of water in the northern-western Sudan. *Journal of Geography, 85*, 412–431.

Shamseldin, A. Y. (1997). Application of a neural network technique to rainfall-runoff modeling. *Journal of Hydrology, 199*, 272–294.

Shata, A. A. (1982). Hydrogeology of the great Nubian Sandstone basin, Egypt. *Quarterly Journal of Engineering Geology, 15*, 127–133.

Sivaraj, R. (2011). A review of selection methods in genetic algorithm. *International Journal of Engineering and Technology, 3*, 3792–3797.

Sonntag, C. (1986). A time-dependent groundwater model for the Eastern Sahara. *Berliner Geowissenshaftliche Abhandlungen, A72*, 124–134.

Spitz, K., & Moreno, J. (1996). *A Practical Guide to Groundwater and Solute Transport Modeling*. New York: Wiley.

Watanabe, K., Kattel, S., Takeuchi, S., & Mahmod, W. E. (2012). Analysis of pore pressure changes due to shafts excavation by using Genetic Algorithm (GA). *Journal of Japan Society of Civil Engineers, 68*, I_193–I_198.